ACS Energy LETTERS

http://pubs.acs.org/journal/aelccp

LETTER

Deciphering How Anion Clusters Govern Lithium Conduction in Glassy Thiophosphate Electrolytes through Machine Learning

Zhimin Chen, Tao Du, Rasmus Christensen, Mathieu Bauchy, and Morten M. Smedskjaer*

Cite This: *ACS Energy Lett.* 2023, 8, 1969–1975

Read Online

ACCESS | Metrics & More | Article Recommendations | Supporting Information

ABSTRACT: Glasses such as lithium thiophosphates (Li_2S-P_2S_5) show promise as solid electrolytes for batteries, but a poor understanding of how the disordered structure affects lithium transport properties limits the development of glassy electrolytes. To address this, we here simulate glassy Li_2S-P_2S_5 electrolytes with varying fractions of polyatomic anion clusters, i.e., $P_2S_6^{4-}$, $P_2S_7^{4-}$, and PS_4^{3-}, using classical molecular dynamics. Based on the determined variation in ionic conductivity, we use a classification-based machine-learning metric termed "softness"—a structural fingerprint that is correlated to the atomic rearrangement probability—to unveil the structural origin of lithium-ion mobility. The softness distribution of lithium ions is highly spatially correlated: that is, the "soft" (high mobility) lithium ions are predominantly found around PS_4^{3-} units, while the "hard" (low mobility) ions are found around $P_2S_6^{4-}$ units. We also show that soft lithium-ion migration requires a smaller energy barrier to be overcome relative to that observed for hard lithium-ion migration.

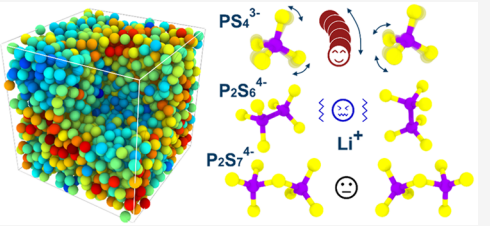

Lithium-ion batteries (LIBs) are an important electrical energy storage technology that has altered the market and direction of electronic devices worldwide.[1−4] However, safety issues and low energy density of the liquid electrolytes used in conventional LIBs are substantial limitations for their future applications.[5−8] All-solid-state batteries (ASSBs) fabricated with solid-state electrolytes (SEs) instead of liquid electrolytes are expected to address these issues.[4,9] SEs are considered to have a strong commercial potential[4,10] and thus replace liquid electrolytes due to their higher energy density,[7] relatively high ionic conductivity at room temperature,[11] high shear modulus to suppress dendrite growth,[10] and nonflammability to improve safety.[12] Such inorganic SEs can be used in various technologies, including solid oxide fuel cells, sensors, and solid-state batteries for electric vehicles.[13] Various studies have reported on the structure and conductivity in inorganic SE material families, such as lanthanide oxides,[14] perovskites,[15] and garnets.[16] Among these, sulfide-based inorganic SEs feature high ionic conductivity, low interfacial resistance to electrodes, and low processing costs, making them some of the most promising inorganic SE materials for ASSBs.[17]

One type of sulfide-based inorganic SE are the lithium thiophosphates, Li_2S-P_2S_5 (LiPS), which constitute a class of thiophosphate LISICON (lithium superionic conductor) that has been widely reported to exhibit high lithium-ion conductivity.[18,19] For example, the ionic conductivity of $70Li_2S$-$30P_2S_5$ glass-ceramic (i.e., partially crystallized glass) reaches 1.7×10^{-2} S cm^{-1} at room temperature,[11] comparable to that of liquid electrolytes. Three predominant anion clusters, $P_2S_6^{4-}$, $P_2S_7^{4-}$, and PS_4^{3-}, are found in Li_2S-P_2S_5 glasses and glass-ceramics. Figure 1A shows these three structures, highlighting the presence of a P−P bond in the $P_2S_6^{4-}$ (*hypo*-thiophosphate) cluster, the corner-sharing $P_2S_7^{4-}$ (*pyro*-thiophosphate) tetrahedral pairs, and the PS_4^{3-} (*ortho*-thiophosphate) tetrahedral cluster. The structure of LiPS glasses and glass-ceramics has been characterized by, e.g., Raman and ^{31}P nuclear magnetic resonance spectroscopy.[20−22] These studies have shown that there are significant differences in the local structures (polyatomic anion) as a function of the glass compositions but also more surprisingly that glasses of the same composition feature different contents of local structures.[23] These structural differences not only occur in LiPS glasses and glass-ceramics prepared by different methods (such as melt-quenching, mechanical ball-milling or heat-treatment), but even in the case of different samples from the same preparation method.

Received: January 31, 2023
Accepted: March 27, 2023
Published: March 29, 2023

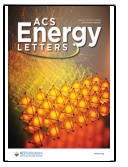

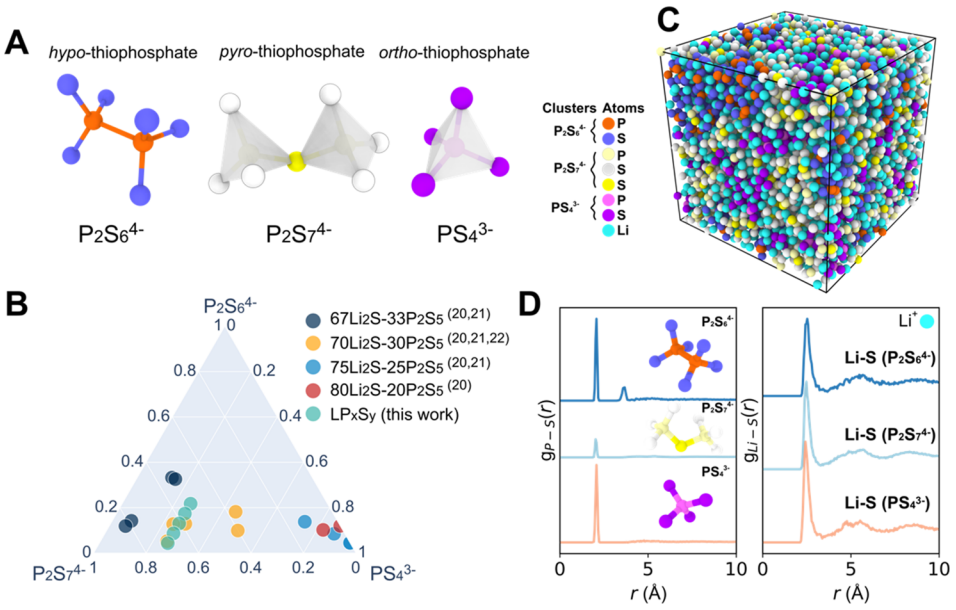

Figure 1. Polyatomic anion clusters in LiPS glassy electrolytes. (A) Schematic illustration of thiophosphate species in LiPS glassy electrolytes. (B) Ternary diagram showing the contents of $P_2S_6^{4-}$, $P_2S_7^{4-}$, and PS_4^{3-} units in the Li_2S-P_2S_5 glass system.[20−22] (C) Atomic snapshot of the simulated structure of $LiP_{0.465}S_{1.605}$ glass. (D) P−S (left) and Li−S (right) partial pair distribution functions $g(r)$.

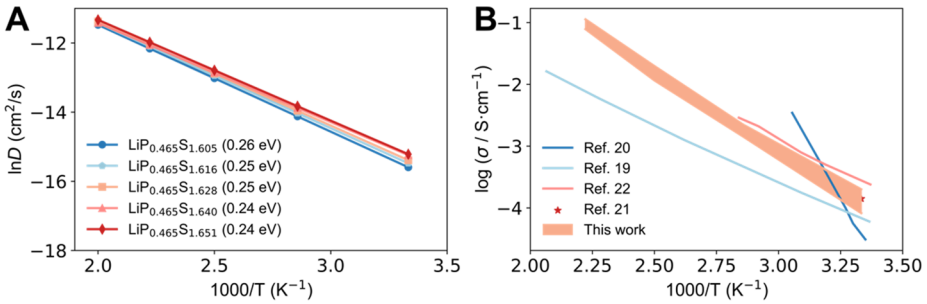

Figure 2. Ionic conductivity of lithium. (A) Temperature dependence of the diffusion coefficient of lithium. The activation energy (stated in parentheses) was calculated from the slope of the Arrhenius fitted plot. (B) Estimated range of ionic conductivity of LiPS glassy electrolytes from this work (orange-colored area), as calculated from the diffusion coefficient via the Nernst−Einstein equation. The results are compared with experimental and simulated ionic conductivity of 70Li_2S-30P_2S_5 glassy electrolytes from the literature with different fractions of polyatomic anion clusters.[20,19,22,21]

The mechanism of the formation and transformation of the different polyatomic anions in LiPS systems is therefore still not well understood. Since these differences cause changes in the performance of LiPS electrolytes, they are important to clarify.[23] While various effects and phenomena in LiPS electrolytes have been investigated, such as the paddle-wheel effect due to the vibration of PS_4^{3-},[24] the suppressive effect of $P_2S_6^{4-}$ on the lithium-ion conductivity,[25] or the uncertain influence of $P_2S_7^{4-}$ on the transport of lithium, few studies have addressed how the content of different polyatomic anion clusters specifically affects the conductive performance of LiPS glassy electrolytes.

In this study, we therefore systematically vary the content of anion clusters in LiPS glasses and investigated its effect on the lithium-ion conduction mechanism. We use a recently developed classical interatomic potential[26] to perform molecular dynamics (MD) simulations of these glassy electrolytes. To analyze the spatial distribution of lithium ions around the polyatomic anion clusters, we use classification-based machine learning to calculate the "softness"[27] of lithium ions around $P_2S_6^{4-}$, $P_2S_7^{4-}$, and PS_4^{3-} from the static structures of LiPS glasses. The mobility and immobility of lithium ions are classified by the softness method, and by also using the nudged elastic band (NEB) method, we estimate the energy landscape along the minimum energy path (MEP)[28] of lithium transport. We demonstrate that softness correlates with the lithium migration capacity and reveal how the fraction of local anion clusters affects the conductivity of lithium ions.

We first summarize the structural information on the LiPS glasses reported in the literature and measured herein (Figure 1B). Compared to the experimental X-ray and neutron diffraction results,[26] the classical MD potential[26] used in this work (see Methods in the Supporting Information for details) reproduces the structure of LiPS glasses very well, at both the short- and medium-range length scales. Besides the classical potential used in this study, another potential has recently been used to study lithium conduction in both LiPS glass and glass-ceramic systems, with special emphasis on the effect of rotation of a single PS_4^{3-} anion on lithium conduction in the Li_3PS_4 system.[29,30] Here, we selected the potential from ref 26, not only because of its accurate reproduction of structural features

https://doi.org/10.1021/acsenergylett.3c00237
ACS Energy Lett. 2023, 8, 1969−1975

as well as ionic conductivity (compared to experiment and *ab initio* MD results[26]) but also more importantly because it allows us to tune the content of local structures in the glasses to match that of the experimentally reported LiPS glassy electrolytes from the literature.

Specifically, we simulated five different $P_2S_6^{4-}$ and $P_2S_7^{4-}$ contents in Li_2S-P_2S_5 glassy electrolyte systems, where the ratio of Li_2S to P_2S_5 is approximately 7:3. The individual cluster contents are also labeled in Figure 1B, and detailed composition information is provided in Table S1 in the Supporting Information. We constructed the glassy electrolyte with the chemical formula LiP_xS_y, where x is equal to 0.465 and y increases from 1.605 to 1.651. The number of lithium atoms was kept constant in the modeling (total system size of ∼8000 atoms containing 2580 lithium atoms). As an example, Figure 1C shows an atomic snapshot of the $LiP_{0.465}S_{1.605}$ glass structure. Depending on the environment in which the different atoms are located, we have calculated the pair distribution functions $g(r)$ that represent the probability of finding an adjacent atom at a distance r from a given atom. $g_{P-S}(r)$. As shown in the left panel of Figure 1D, the lengths of the P−S bonds are in the range of ∼2.1 Å for all three clusters, and in $P_2S_6^{4-}$, the distance between P and S bonded to its neighboring P is concentrated in the range of 3.4−3.8 Å due to the presence of P−P bonds. The right panel of Figure 1D depicts the pair distribution functions of Li−S in $P_2S_6^{4-}$, $P_2S_7^{4-}$, and PS_4^{3-}, finding no differences in the distance between Li and S. That is, Li is uniformly distributed around these three clusters.

As we have varied the relative content of $P_2S_6^{4-}$, $P_2S_7^{4-}$, and PS_4^{3-} anions in the LiPS glassy electrolytes, the conduction propensity of lithium ions changes accordingly. Figure 2A presents the temperature dependence of the diffusion coefficient of lithium ions (as determined from mean square displacement; see Methods in the Supporting Information). The data follow Arrhenius kinetics, with a decrease in the activation energy due to the decrease in the content of $P_2S_6^{4-}$ in the system. We also note a weakening of the lithium diffusion capacity due to the absence of S, i.e., an increased activation energy, suggesting that the reduction of P−S bonds, which is attributed to the relatively higher fraction of $P_2S_6^{4-}$ in the system, may impede the lithium conduction.

Based on the diffusion coefficient, the Nernst−Einstein equation (see eq 4 in the Supporting Information) was used to calculate the ionic conductivity of lithium. The orange-colored area in Figure 2B shows the ionic conductivity of the present LiPS glassy electrolyte compared with experimental data from the literature.[20,19,22,21] Interestingly, the ionic conductivity in the $70Li_2S$-$30P_2S_5$ glass system shows significant variations as presented in Figure 2B, owing to the different contents of $P_2S_6^{4-}$, $P_2S_7^{4-}$, and PS_4^{3-} (as shown in Figure 1B). The rotational dynamics of the PS_4^{3-} units have previously been proven to promote the migration of lithium ions, which is known as the paddle-wheel effect.[24] The $P_2S_6^{4-}$ units are considered to be unstable structures,[31] and the combination of small intrinsic defect concentrations and relatively high migration barriers results in very low theoretical lithium ion conductivity for the $Li_4P_2S_6$ crystal.[25] In the case of the present glasses, which lack long-range order, a robust transport pathway for lithium in the vicinity of $P_2S_6^{4-}$ may be hindered by intricate $P_2S_6^{4-}$ displacements. The increase in activation energy and decrease in ionic conductivity observed with increasing fraction of $P_2S_6^{4-}$ also suggest a possible mechanism for hindrance caused by $P_2S_6^{4-}$. In early studies,[21,32,33] it has been proposed that the corner-sharing $P_2S_7^{4-}$ units shield the positive charge of P due to the electron transfer between P and the bridging S, thus suppressing Li conduction. In addition, another study found that the flexibility of the $P_2S_7^{4-}$ ditetrahedra promote the diffusion of Li ions.[34] In the present study, the fraction of $P_2S_7^{4-}$ varies inversely and synchronously with $P_2S_6^{4-}$, and the observed monotonic changes in ionic conductivity cannot be solely attributed to either of them, including PS_4^{3-}. The disordered and complex distribution of polyatomic anion clusters in such glasses necessitates the use of advanced computational methods to elucidate the mechanism of lithium conduction under the influence of localized structures.

Next, we therefore attempt to decipher how the spatial environment around the $P_2S_6^{4-}$, $P_2S_7^{4-}$, and PS_4^{3-} anions affect the lithium transport in the present glasses. To this end, we correlate the local structure and dynamics by using the "softness"[27,35−37] concept, which is based on classification-based machine learning to investigate the relationship between the mobility of lithium and the local environment in which it is located. Specifically, we use logistic regression[38] to build a hyperplane (that separates "mobile" from "immobile" lithium ions) based on the static structure and corresponding rearrangement of each lithium atom at 300 K as obtained from the MD simulations to identify their mobility. We also calculate the nonaffine square displacement D^2_{min} of each lithium ion, as this property has been widely used to describe the atomic rearrangement processes. The rearrangement degree of each lithium ion is quantified by the sum of D^2_{min} values during small increments of time (D_{cum}). Details of these calculations are given in the Supporting Information.

We find that the accuracy of the lithium mobility classification exceeds 70% for both the test sets and training sets when relying solely on the radial structure function of lithium with other atom pairs, as shown in Figure S1 in the Supporting Information. The established hyperplane divides all lithium ions into mobile (soft) or immobile (hard), as associated with positive and negative values of S, respectively. The magnitude of the distance from the hyperplane represents the magnitude of the absolute value of the softness for lithium. Figure 3A shows the snapshot of the spatial softness distribution of all lithium atoms in the $LiP_{0.465}S_{1.605}$ sample as an example (Figure S2 in the Supporting Information provides the snapshots of all samples). In contrast to crystalline materials with specific ion transport channels,[39] the complex local structure in glass allows for diverse mobility of lithium. Figure 3B shows the distribution of softness in glasses with different anion cluster contents, showing that the peak shifts toward higher softness with decreasing $P_2S_6^{4-}$ content and increasing $P_2S_7^{4-}$ content in the structure.

Considering that the local environment around lithium ions should be related to their propensity to conduct, we here propose a correlation between the softness of lithium and its surrounding polyatomic anion clusters, as visualized in Figure 3C. Comparing with Figure 3A, we find that the softness of lithium around PS_4^{3-} is mostly positive while that around $P_2S_6^{4-}$ is mostly negative, with strong spatial correlation between them. The Pearson product-moment correlation coefficients between the softness value of Li and the probability of finding S atoms in $P_2S_6^{4-}$ clusters surrounding that Li atoms is about −96% and is over +96% for Li-PS_4^{3-}. To validate this observation, we have calculated the pair distribution function of Li−S (S in the different anion clusters) as shown in Figure

https://doi.org/10.1021/acsenergylett.3c00237
ACS Energy Lett. 2023, 8, 1969−1975

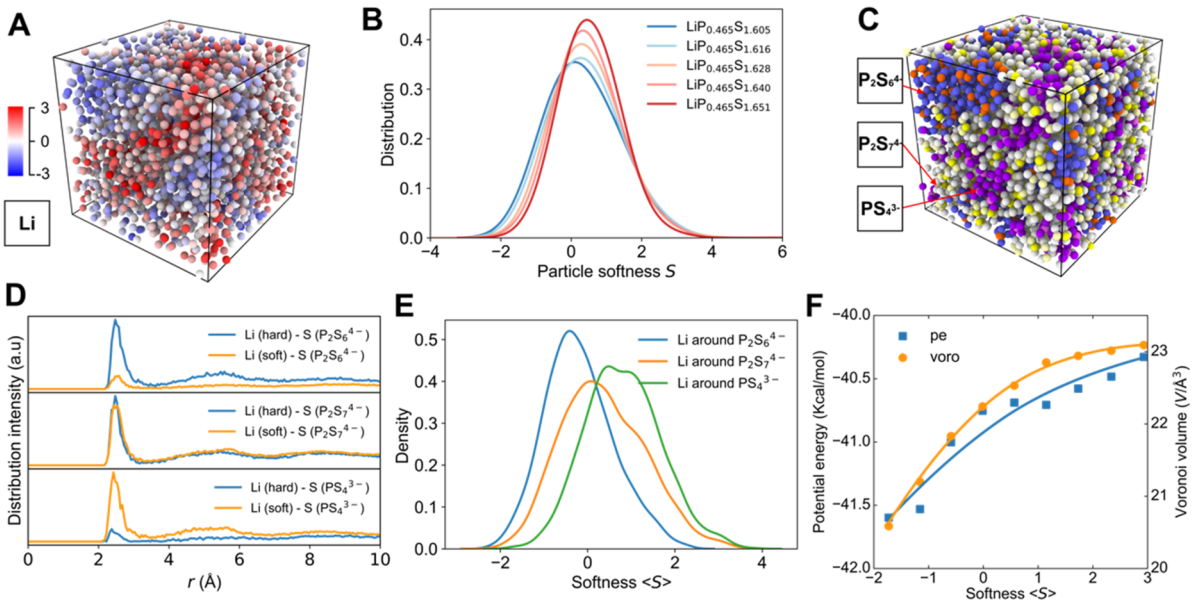

Figure 3. Classification-based machine-learning analysis of lithium mobility. (A) Atomic snapshot of lithium ions in the $LiP_{0.465}S_{1.605}$ glass, where the lithium ions are color-coded by their local softness value. (B) Particle softness distribution of lithium in different LiPS glassy electrolytes. (C) Polyatomic anion cluster distribution in the glass structure of $LiP_{0.465}S_{1.605}$ with all lithium ions hidden for a better visualization and comparison. Note that the snapshots in panels (A) and (C) are exported from the same simulated $LiP_{0.465}S_{1.605}$ glass structure. (D) Partial radial distribution function of Li−S pairs in the $LiP_{0.465}S_{1.605}$ sample as calculated separately for S atoms in different polyatomic anion clusters. Soft and hard lithium ions in the Li−S pairs are colored blue and orange, respectively. (E) Particle softness distribution of lithium around different polyatomic anion clusters within 5 Å (shown for $LiP_{0.465}S_{1.605}$ as an example). (F) Potential energy (pe, kcal/mol) and Voronoi volume (voro, Å^3) of lithium ions as a function of their particle softness. The solid lines are guides to the eye.

3D, which represents the probability of finding a neighboring S in $P_2S_6^{4-}$, $P_2S_7^{4-}$, or PS_4^{3-} at a distance r from a given Li atom. The results are shown in Figure 3E, which further identifies the exact particle softness distribution of lithium around different anion clusters, showing that softness can be used to identify the mobility of lithium and confirming the strong correlation between lithium mobility and its local environment. Here, it should be stressed that the softness is only calculated from the surrounding Li, not the neighboring P and S atoms. In other words, the anion clusters impact the spatial distribution of the Li around them, which, in turn, governs the mobility of Li atoms. Furthermore, we find that the potential energy and Voronoi volume of lithium ions are also strongly related to their softness as presented in Figure 3F: that is, the lithium atoms with larger softness tend to have a higher potential energy and Voronoi volume. This is as expected, considering that both local free volume (high Voronoi volume) and instability (high energy) should promote the mobility of Li atoms.

We have demonstrated above that Li ions around PS_4^{3-} have a high mobility, while the presence of $P_2S_6^{4-}$ units has a strong negative effect on the mobility of Li. In the following, we further investigate the relationship between softness and the migration capacity of lithium. The ionic diffusion in the solid state can be described as the hopping of individual ions between ground-state stable sites and/or intermediate metastable sites of the crystal structural framework constituted of anions (for example, O^{2-}, S^{2-}, or polyatomic anion clusters).[8,39] The absence of regular coordination sites and symmetric long-range migration pathways in disordered materials makes it difficult to establish the conduction theory, but the hopping theory of a mobile element can still be utilized. To this end, a statistical analysis is needed to calculate the energy barrier distribution of hopping ions in disordered materials, instead of considering a discrete one resembling that in a crystalline material.[8] Therefore, we have performed classical molecular dynamics simulations in this work (instead of *ab initio* MD), as they allow us to obtain glass structures with thousands (instead of hundreds) of atoms.

As illustrated in Figure 4A, the ion migrates through the energy landscape, and the highest point of the energy landscape along the migration path dictates the energy barrier for its diffusion. Here, the energy landscape of each lithium is captured by using the nudged elastic band (NEB) method, which has been widely used to identify the minimum energy path (MEP) and thus the energy barrier across which each lithium ion migrates over when it migrates to another lithium site (5−10 Å away). We classify lithium into two categories according to the softness values, i.e., hard lithium ($S < 0$) and soft lithium ($S > 0$). Figure S3 in the Supporting Information shows the energy barrier distribution for all lithium migrations, with soft lithium ions requiring lower energy barriers to be overcome than those of hard lithium ions. Calculation of the lithium migration barrier considering only the softness of the lithium at the initial site leads to an underestimation of the discrepancy in the distribution: that is, a slight shift in the distribution of energy barriers as observed from Figure S3.

To this end, we have also calculated the energy barrier that needs to be overcome for lithium to migrate to lithium sites with the opposite softness values (i.e., a soft lithium migrating to hard lithium sites, or vice versa). Figure 4B exemplifies the energy landscape of a single lithium migration. Combined with the energy barrier distribution in Figure 4C, we find that soft lithium ions require a smaller energy barrier to be overcome to migrate to another site, indicating that soft lithium ions are more mobile and are in a relatively high energy state, while

https://doi.org/10.1021/acsenergylett.3c00237
ACS Energy Lett. 2023, 8, 1969−1975

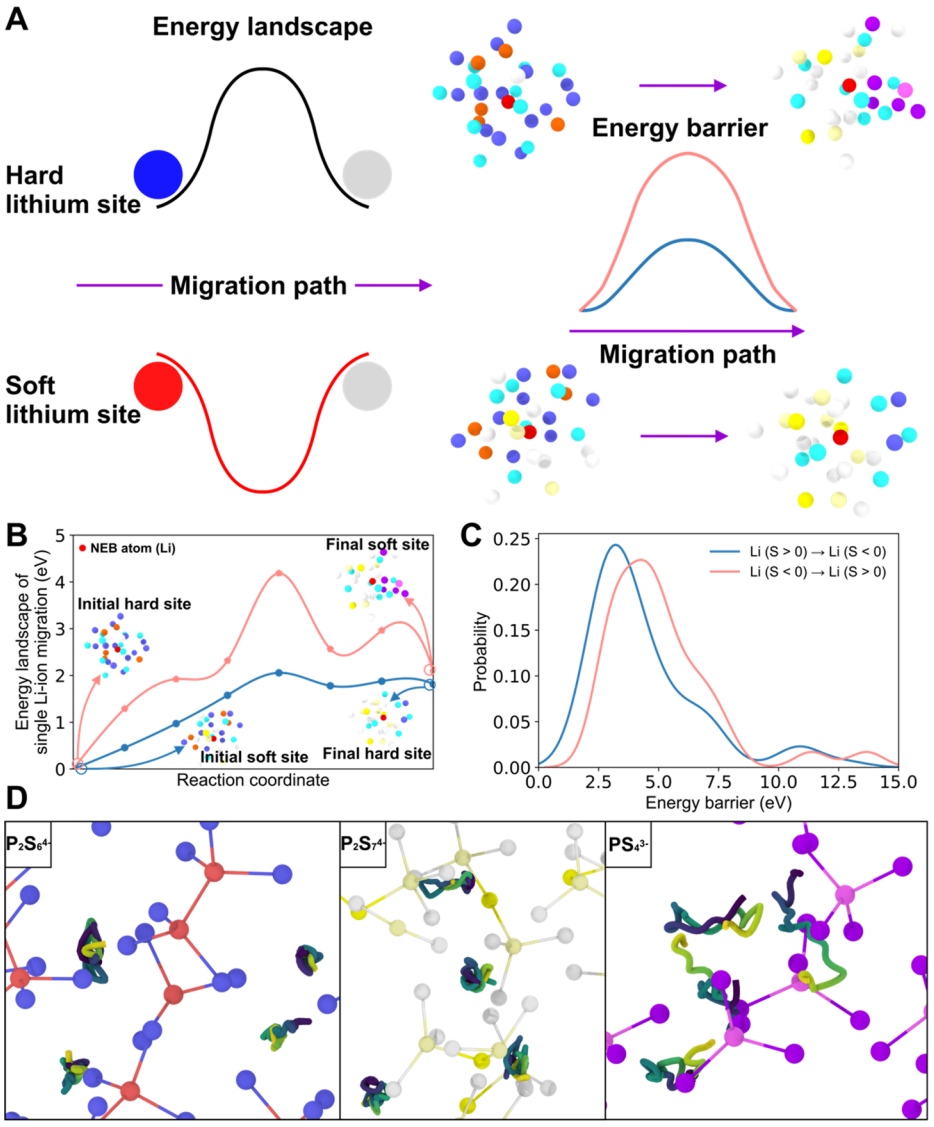

Figure 4. Lithium-ion diffusion mechanism. (A) Schematic illustration of single Li-ion migration. (B) Energy landscape of a single Li-ion migration from an initial soft (hard) position to the final hard (soft) site taking $LiP_{0.465}S_{1.605}$ glass as an example. (C) Energy barrier distribution for lithium migration. (D) Lithium's trajectory trace over 10 ps of simulation time at 500 K in the $LiP_{0.465}S_{1.605}$ glass, where dark green and bright green correspond to the initial and final positions, respectively.

hard lithium ions tend to be caged by the surrounding local environment and require more energy to migrate out. By tracing the trajectories of lithium atoms around different anion clusters over 10 ps at 500 K, as shown in Figure 4D, we can observe that the lithium ions move locally around $P_2S_6^{4-}$, suppressing the lithium mobility due to the relatively larger energy barrier, while the lithium ions around PS_4^{3-} tend to be enhanced and undergo a long hopping event. We also observe that the lithium ions surrounding $P_2S_7^{4-}$ exhibit limited long-range mobility, and considering the near-zero softness value of the lithium ions around these units, we infer that their impact on lithium transport is likely insignificant.

Understanding the spatial distribution of lithium ions and their location relative to structural features, i.e., medium-range order (MRO) structural information such as rings, is important for resolving the factors influencing the ionic conductivity. To this end, we have used persistent homology as introduced in Methods and Supporting Text. The first sharp diffraction peak (FSDP) of the structure factor is typically considered to be the signature of MRO in glasses. Here, we find that it can be assigned to rings with a size above 8 (Figure S4 in the Supporting Information). These rings are composed of S atoms, or P and S atoms, coming from $P_2S_6^{4-}$, $P_2S_7^{4-}$, and PS_4^{3-}, which represent a complex chemical environment in the glass structure as schematically illustrated in Figure S5a. The ring size dependency of lithium softness distribution shows a similar distribution to the total softness of lithium as shown in Figures S5b–e. As it may be expected that the MRO topology could have only a second-order effect on lithium-ion mobility in addition to the first-order effect of softness, we have performed analyses to clarify whether these MRO structures may have any impact on the mobility resulting from the formation of free volumes, transport channels, etc. owing to special topology. However, we do not find that kind of correlation between the softness of the lithium around the ring and the MRO topology of the LiPS glassy electrolytes (see Supporting Text).

https://doi.org/10.1021/acsenergylett.3c00237
ACS Energy Lett. 2023, 8, 1969−1975

In summary, we have constructed Li_2S-P_2S_5 glasses with different polyatomic anion cluster fractions using classical molecular dynamics simulations and observed the variation of their ionic conductivity. The findings show that the local environment in which the lithium ions are located affects their conduction properties. To unravel the complicated chemical environment in which the lithium ions are located, we have used logistic-regression-based machine learning to extract the "softness" information on lithium ions as it is encoded in their spontaneous dynamics, describing the mobility (soft) and immobility (hard) of lithium. We find a significant spatial softness distribution of lithium: namely, hard lithium is distributed around $P_2S_6^{4-}$, soft lithium is distributed around PS_4^{3-}, and the softness values of lithium around $P_2S_7^{4-}$ are mostly around zero. The positive correlation between the softness of lithium and its potential energy and Voronoi volume is further demonstrated. We also find that the lithium ions with higher softness have a smaller migration energy barrier, and it is thus easier for them to diffuse. On the other hand, the hard lithium ions are caged in their local environment and require higher energy to become activated.

■ ASSOCIATED CONTENT

Supporting Information

The Supporting Information is available free of charge at https://pubs.acs.org/doi/10.1021/acsenergylett.3c00237.

Details on sample preparation via MD simulation, diffusion and rearrangement of lithium calculations, machine-learning modeling, NEB method, persistent homology calculation, medium-range order structure analysis, and an additional table and figures (PDF)

■ AUTHOR INFORMATION

Corresponding Author

Morten M. Smedskjaer − *Department of Chemistry and Bioscience, Aalborg University, Aalborg East 9220, Denmark;* orcid.org/0000-0003-0476-2021; Email: mos@bio.aau.dk

Authors

Zhimin Chen − *Department of Chemistry and Bioscience, Aalborg University, Aalborg East 9220, Denmark*

Tao Du − *Department of Chemistry and Bioscience, Aalborg University, Aalborg East 9220, Denmark*

Rasmus Christensen − *Department of Chemistry and Bioscience, Aalborg University, Aalborg East 9220, Denmark*

Mathieu Bauchy − *Department of Civil and Environmental Engineering, University of California, Los Angeles, California 90095, United States;* orcid.org/0000-0003-4600-0631

Complete contact information is available at: https://pubs.acs.org/10.1021/acsenergylett.3c00237

Author Contributions

M.M.S. conceived and supervised the study. Z.C. and M.M.S. planned the computational work. Z.C. performed the molecular dynamics simulations, structural analyses, and machine-learning calculations, with input and assistance from T.D., R.C., and M.B. Z.C. and M.M.S. wrote the manuscript, with revisions from M.B., T.D., and R.C. All authors participated in discussing the data.

Notes

The authors declare no competing financial interest.

■ ACKNOWLEDGMENTS

This work was supported by grants from the China Scholarship Council (202106880010), a Marie Skłodowska-Curie Individual Fellowship (101018156), Independent Research Fund Denmark (1127-00003), and the Danish Data Science Academy, which is funded by the Novo Nordisk Foundation (NNF21SA0069429) and VILLUM FONDEN (40516). We also acknowledge the computational resources supplied by Danish e-infrastructure Cooperation (DeiC) National HPC (DeiC-AAU-N5-202200005) and Aalborg University (CLAAUDIA). M.B. acknowledges funding provided by the National Science Foundation under grants DMR-1944510 and DMR-1928538.

■ REFERENCES

(1) Chu, S.; Majumdar, A. Opportunities and Challenges for a Sustainable Energy Future. *Nature* **2012**, *488* (7411), 294−303.

(2) Liu, H.; Cheng, X.-B.; Huang, J.-Q.; Yuan, H.; Lu, Y.; Yan, C.; Zhu, G.-L.; Xu, R.; Zhao, C.-Z.; Hou, L.-P.; He, C.; Kaskel, S.; Zhang, Q. Controlling Dendrite Growth in Solid-State Electrolytes. *ACS Energy Lett.* **2020**, *5* (3), 833−843.

(3) Dawson, J. A.; Canepa, P.; Famprikis, T.; Masquelier, C.; Islam, M. S. Atomic-Scale Influence of Grain Boundaries on Li-Ion Conduction in Solid Electrolytes for All-Solid-State Batteries. *J. Am. Chem. Soc.* **2018**, *140* (1), 362−368.

(4) Sarkar, S.; Thangadurai, V. Critical Current Densities for High-Performance All-Solid-State Li-Metal Batteries: Fundamentals, Mechanisms, Interfaces, Materials, and Applications. *ACS Energy Lett.* **2022**, *7* (4), 1492−1527.

(5) Goodenough, J. B.; Kim, Y. Challenges for Rechargeable Li Batteries. *Chem. Mater.* **2010**, *22* (3), 587−603.

(6) Zheng, Y.; Yao, Y.; Ou, J.; Li, M.; Luo, D.; Dou, H.; Li, Z.; Amine, K.; Yu, A.; Chen, Z. A Review of Composite Solid-State Electrolytes for Lithium Batteries: Fundamentals, Key Materials and Advanced Structures. *Chem. Soc. Rev.* **2020**, *49* (23), 8790−8839.

(7) Janek, J.; Zeier, W. G. A Solid Future for Battery Development. *Nat. Energy* **2016**, *1* (9), 16141.

(8) Famprikis, T.; Canepa, P.; Dawson, J. A.; Islam, M. S.; Masquelier, C. Fundamentals of Inorganic Solid-State Electrolytes for Batteries. *Nat. Mater.* **2019**, *18* (12), 1278−1291.

(9) Shen, C.; Huang, Y.; Yang, J.; Chen, M.; Liu, Z. Unraveling the Mechanism of Ion and Electron Migration in Composite Solid-State Electrolyte Using Conductive Atomic Force Microscopy. *Energy Storage Materials* **2021**, *39*, 271−277.

(10) Boaretto, N.; Garbayo, I.; Valiyaveettil-SobhanRaj, S.; Quintela, A.; Li, C.; Casas-Cabanas, M.; Aguesse, F. Lithium Solid-State Batteries: State-of-the-Art and Challenges for Materials, Interfaces and Processing. *J. Power Sources* **2021**, *502*, No. 229919.

(11) Seino, Y.; Ota, T.; Takada, K.; Hayashi, A.; Tatsumisago, M. A Sulphide Lithium Super Ion Conductor Is Superior to Liquid Ion Conductors for Use in Rechargeable Batteries. *Energy Environ. Sci.* **2014**, *7* (2), 627−631.

(12) Zhang, Z.; Shao, Y.; Lotsch, B.; Hu, Y.-S.; Li, H.; Janek, J.; Nazar, L. F.; Nan, C.-W.; Maier, J.; Armand, M.; Chen, L. New Horizons for Inorganic Solid State Ion Conductors. *Energy Environ. Sci.* **2018**, *11* (8), 1945−1976.

(13) Bachman, J. C.; Muy, S.; Grimaud, A.; Chang, H.-H.; Pour, N.; Lux, S. F.; Paschos, O.; Maglia, F.; Lupart, S.; Lamp, P.; Giordano, L.; Shao-Horn, Y. Inorganic Solid-State Electrolytes for Lithium Batteries: Mechanisms and Properties Governing Ion Conduction. *Chem. Rev.* **2016**, *116* (1), 140−162.

(14) Adachi, G.; Imanaka, N.; Tamura, S. Ionic Conducting Lanthanide Oxides. *Chem. Rev.* **2002**, *102* (6), 2405−2430.

(15) Bohnke, O.; Bohnke, C.; Fourquet, J. L. Mechanism of Ionic Conduction and Electrochemical Intercalation of Lithium into the Perovskite Lanthanum Lithium Titanate. *Solid State Ionics* **1996**, *91* (1), 21−31.

(16) Thangadurai, V.; Narayanan, S.; Pinzaru, D. Garnet-Type Solid-State Fast Li Ion Conductors for Li Batteries: Critical Review. *Chem. Soc. Rev.* **2014**, *43* (13), 4714−4727.
(17) Garcia-Mendez, R.; Smith, J. G.; Neuefeind, J. C.; Siegel, D. J.; Sakamoto, J. Correlating Macro and Atomic Structure with Elastic Properties and Ionic Transport of Glassy Li_2S-P_2S_5 (LPS) Solid Electrolyte for Solid-State Li Metal Batteries. *Adv. Energy Mater.* **2020**, *10* (19), No. 2000335.
(18) Liu, Z.; Fu, W.; Payzant, E. A.; Yu, X.; Wu, Z.; Dudney, N. J.; Kiggans, J.; Hong, K.; Rondinone, A. J.; Liang, C. Anomalous High Ionic Conductivity of Nanoporous β-Li_3PS_4. *J. Am. Chem. Soc.* **2013**, *135* (3), 975−978.
(19) Mizuno, F.; Hayashi, A.; Tadanaga, K.; Tatsumisago, M. New, Highly Ion-Conductive Crystals Precipitated from Li_2S-P_2S_5 Glasses. *Adv. Mater.* **2005**, *17* (7), 918−921.
(20) Dietrich, C.; Weber, D. A.; Sedlmaier, S. J.; Indris, S.; Culver, S. P.; Walter, D.; Janek, J.; Zeier, W. G. Lithium Ion Conductivity in Li_2S-P_2S_5 Glasses − Building Units and Local Structure Evolution during the Crystallization of Superionic Conductors Li_3PS_4, $Li_7P_3S_{11}$ and $Li_4P_2S_7$. *J. Mater. Chem. A* **2017**, *5* (34), 18111−18119.
(21) Ohara, K.; Mitsui, A.; Mori, M.; Onodera, Y.; Shiotani, S.; Koyama, Y.; Orikasa, Y.; Murakami, M.; Shimoda, K.; Mori, K.; Fukunaga, T.; Arai, H.; Uchimoto, Y.; Ogumi, Z. Structural and Electronic Features of Binary Li_2S-P_2S_5 Glasses. *Sci. Rep* **2016**, *6* (1), 21302.
(22) Uchida, K.; Ohkubo, T.; Utsuno, F.; Yazawa, K. Modified $Li_7P_3S_{11}$ Glass-Ceramic Electrolyte and Its Characterization. *ACS Appl. Mater. Interfaces* **2021**, *13* (31), 37071−37081.
(23) Preefer, M. B.; Grebenkemper, J. H.; Wilson, C. E.; Everingham, M.; Cooley, J. A.; Seshadri, R. Subtle Local Structural Details Influence Ion Transport in Glassy Li^+ Thiophosphate Solid Electrolytes. *ACS Appl. Mater. Interfaces* **2021**, *13* (48), 57567−57575.
(24) Smith, J. G.; Siegel, D. J. Low-Temperature Paddlewheel Effect in Glassy Solid Electrolytes. *Nat. Commun.* **2020**, *11* (1), 1483.
(25) Dietrich, C.; Sadowski, M.; Sicolo, S.; Weber, D. A.; Sedlmaier, S. J.; Weldert, K. S.; Indris, S.; Albe, K.; Janek, J.; Zeier, W. G. Local Structural Investigations, Defect Formation, and Ionic Conductivity of the Lithium Ionic Conductor $Li_4P_2S_6$. *Chem. Mater.* **2016**, *28* (23), 8764−8773.
(26) Ariga, S.; Ohkubo, T.; Urata, S.; Imamura, Y.; Taniguchi, T. A New Universal Force-Field for the Li_2S-P_2S_5 System. *Phys. Chem. Chem. Phys.* **2022**, *24* (4), 2567−2581.
(27) Schoenholz, S. S.; Cubuk, E. D.; Sussman, D. M.; Kaxiras, E.; Liu, A. J. A Structural Approach to Relaxation in Glassy Liquids. *Nature Phys.* **2016**, *12* (5), 469−471.
(28) Zarkevich, N. A.; Johnson, D. D. Nudged-Elastic Band Method with Two Climbing Images: Finding Transition States in Complex Energy Landscapes. *J. Chem. Phys.* **2015**, *142* (2), No. 024106.
(29) Forrester, F. N.; Quirk, J. A.; Famprikis, T.; Dawson, J. A. Disentangling Cation and Anion Dynamics in Li_3PS_4 Solid Electrolytes. *Chem. Mater.* **2022**, *34* (23), 10561−10571.
(30) Kim, J.-S.; Jung, W. D.; Son, J.-W.; Lee, J.-H.; Kim, B.-K.; Chung, K.-Y.; Jung, H.-G.; Kim, H. Atomistic Assessments of Lithium-Ion Conduction Behavior in Glass−Ceramic Lithium Thiophosphates. *ACS Appl. Mater. Interfaces* **2019**, *11* (1), 13−18.
(31) Sadowski, M.; Albe, K. Computational Study of Crystalline and Glassy Lithium Thiophosphates: Structure, Thermodynamic Stability and Transport Properties. *J. Power Sources* **2020**, *478*, No. 229041.
(32) Mori, K.; Enjuji, K.; Murata, S.; Shibata, K.; Kawakita, Y.; Yonemura, M.; Onodera, Y.; Fukunaga, T. Direct Observation of Fast Lithium-Ion Diffusion in a Superionic Conductor: $Li_7P_3S_{11}$ Metastable Crystal. *Phys. Rev. Applied* **2015**, *4* (5), No. 054008.
(33) Mori, K.; Ichida, T.; Iwase, K.; Otomo, T.; Kohara, S.; Arai, H.; Uchimoto, Y.; Ogumi, Z.; Onodera, Y.; Fukunaga, T. Visualization of Conduction Pathways in Lithium Superionic Conductors: Li_2S-P_2S_5 Glasses and $Li_7P_3S_{11}$ Glass−Ceramic. *Chem. Phys. Lett.* **2013**, *584*, 113−118.
(34) Chu, I.-H.; Nguyen, H.; Hy, S.; Lin, Y.-C.; Wang, Z.; Xu, Z.; Deng, Z.; Meng, Y. S.; Ong, S. P. Insights into the Performance Limits of the $Li_7P_3S_{11}$ Superionic Conductor: A Combined First-Principles and Experimental Study. *ACS Appl. Mater. Interfaces* **2016**, *8* (12), 7843−7853.
(35) Liu, H.; Xiao, S.; Tang, L.; Bao, E.; Li, E.; Yang, C.; Zhao, Z.; Sant, G.; Smedskjaer, M. M.; Guo, L.; Bauchy, M. Predicting the Early-Stage Creep Dynamics of Gels from Their Static Structure by Machine Learning. *Acta Mater.* **2021**, *210*, No. 116817.
(36) Du, T.; Liu, H.; Tang, L.; Sørensen, S. S.; Bauchy, M.; Smedskjaer, M. M. Predicting Fracture Propensity in Amorphous Alumina from Its Static Structure Using Machine Learning. *ACS Nano* **2021**, *15* (11), 17705−17716.
(37) Cubuk, E. D.; Ivancic, R. J. S.; Schoenholz, S. S.; Strickland, D. J.; Basu, A.; Davidson, Z. S.; Fontaine, J.; Hor, J. L.; Huang, Y.-R.; Jiang, Y.; Keim, N. C.; Koshigan, K. D.; Lefever, J. A.; Liu, T.; Ma, X.-G.; Magagnosc, D. J.; Morrow, E.; Ortiz, C. P.; Rieser, J. M.; Shavit, A.; Still, T.; Xu, Y.; Zhang, Y.; Nordstrom, K. N.; Arratia, P. E.; Carpick, R. W.; Durian, D. J.; Fakhraai, Z.; Jerolmack, D. J.; Lee, D.; Li, J.; Riggleman, R.; Turner, K. T.; Yodh, A. G.; Gianola, D. S.; Liu, A. J. Structure-Property Relationships from Universal Signatures of Plasticity in Disordered Solids. *Science* **2017**, *358* (6366), 1033−1037.
(38) Liu, H.; Smedskjaer, M. M.; Bauchy, M. Deciphering a Structural Signature of Glass Dynamics by Machine Learning. *Phys. Rev. B* **2022**, *106* (21), No. 214206.
(39) He, X.; Zhu, Y.; Mo, Y. Origin of Fast Ion Diffusion in Super-Ionic Conductors. *Nat. Commun.* **2017**, *8* (1), 15893.

https://doi.org/10.1021/acsenergylett.3c00237
ACS Energy Lett. 2023, 8, 1969−1975